Control Strategy of PMSG Generator in Small Wind Turbine System

Abdelkader HARROUZ[1,*], Ilhami COLAK[2] , Korhan KAYISILI[2]

[1]Department of Hydrocarbon and Renewable Energy, Faculty of Science and Technology, University of Ahmed Draïa, Adrar, Algeria

[2]Department of Electrical Electronics Eng., Faculty of Engineering Architecture, Nisantasi University, Istanbul, Turkey

[*]Corresponding author; Email: abd.harrouz@univ-adrar.dz.

Article Info

Article history:

Received May 12, 2022
Revised June 10, 2022
Accepted June 13, 2022

Keywords:

Vector control
Small wind
Permanent-magnet synchronous generator PMSG
FOC
MPPT control
DC bus
Buck converter
DPC

ABSTRACT

This paper presents a control strategy of turbine directly driven permanent magnet synchronous generator (PMSG) for a small wind generation system. The mathematical models of a wind turbine system, the PMSG generator and converters have been described. The control algorithms of the converter systems based on the methods of vector control have been applied. The study methodology is based on defining various study cases combining structural and operational parameters of the wind energy systems. The models of the PMSG, the force commutated rectifier, the DC bus, the buck converter and the inverter are developed and used in the control scheme. The objective of this paper is to compare between tow controls with simulation, and with more description of all the system by developing the technique needed to control the converter. The simulation results will show that the proposed control can operate with a good performance in a stand-alone wind energy conversion system for low power generation applications.

I. Introduction

Recently, with technological advancement, wind power has grown rapidly and becomes the most competitive form of renewable energy resource [1, 2]. The wind energy sector has experienced strong growth in recent years. The development and research are mainly on the side of large wind turbines. These wind turbines are grouped into wind farms at sea or on land, and are connected to the electricity distribution networks. They have blades measuring several tens of meters and a power of the order of megawatt. On the other side of the spectrum are the small-scale wind turbines, with power ratings from 100 watts to tens of kilowatts, which are intended to isolated network production. They are mainly used to power too remote facilities of the electricity distribution network: shelters, cabins, telecommunication stations and sailboats for example [3, 4]. The poor performance of small wind turbines in battery charging applications (Figure 1) is due to proposed configurations and stratigraphic controls applied to increase the output power of wind turbines [5, 6]. The controls of wind turbine system are to improve their service life of energy production.

The objectives of controlling a wind energy system: avoid damage to the wind turbine or the load and maximize energy production. In the past, these small systems have generally been designed to be robust, with robust mechanical controls and relatively modest overall performance. [5, 6, 7].

Due to the advances in microcontrollers, electronics power and wind system penetration, the improvement of control strategies becomes a major challenge for manufacturers in order to comply with the charge requirements [7, 8, 9].

In this context, this paper proposes a control strategy of PMSG wind energy generation system, and discusses back-to-back PWM converter control method and DPC .The scheme of the wind turbine system is shown in Figure 2

Figure .1 Small wind energy application.

The studied system consists of a controlled voltage source rectifier (Vdc). Control strategies based on direct power and vector control are studied for normal and distorted operating conditions [10-12]. The control techniques of the permanent magnet synchronous generator are aimed at controlling the charging current and voltage. On the other hand, the control strategies of the PMSG aim to decouple the active and reactive power supplied to the load. In the literature, different controlling can be seen [12-17]. To achieve these objectives, vector control techniques require a current control, in the rotating reference system, and a decoupling between the components so that the electromagnetic torque and the power are controlled indirectly. In direct DPC power control strategies, the first step is to estimate the torque and power. These two variables are then controlled directly [18].

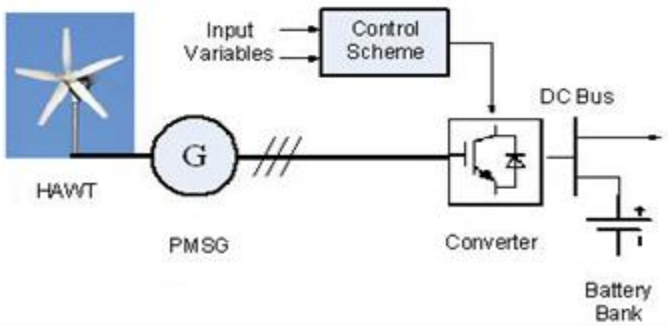

Figure .2 Control of small wind turbine.

For both techniques, the advanced controller part was not taken into account. However, they give very good control results, but the performance study was explored for a small wind turbine [19].

Therefore, in this work, the FOC and DPC control strategies for the generator-side converter are considered. In the first section, the wind turbine model is presented. The second section presents the control strategies of the generator-side converter. The performance of both control techniques is simulated and analyzed [20].

The Permanent Magnet Synchronous Generator “PMSG”, are becoming popular for variable-speed generation system and the use of the PMSG in large wind turbine generators is growing rapidly. It is connected directly to the turbine and so it can operate at low speeds.

For illustration, the figure 3 shows simple and reliable permanent magnet synchronous generators for direct-drive applications (50-300rpm) [20-22].

Figure .3 PMSG generator for wind turbines industrial [23].

The advantage of the permanent magnet machine design is that it has a much higher efficiency (97 %) than the induction machine (85%). Due to their excellent performance especially, efficiency and reliability, the general trend in wind industry is to go for higher powers, which is especially relevant with harsh environment [23].

The aim of this paper is to compared between an intelligent two controls of small wind turbine systems based of PMSG, DPC and PI classic with SVM, to get the best benefit from the wind, and improve performances with low cost.

II. Wind turbine model

The proposed topology is well suited for a low power DC system with battery storage. Along with the electrical generator, the principal electric component of the proposed wind energy system is the proposed DC/DC converter.

Controllability of the system voltage allows the machine rotational speed adjustment to obtain the maximal wind turbine available power.

The wind profile can be modelled by, [2, 5, 7, 10, 13, and 17]:

$$V_{wind}(t) = V_1(1+\sum_i A_i \sin(w_i.t)) \qquad (1)$$

where V1: is the value initial of wind, Ai: is amplitude of wind form, wi : frequency of wind form.

The wind turbine collects the kinetic energy of the wind and converts it into a torque, which turns the blades of the rotor [13]. The machine functions as a generator when it is driven byan external prime mover, like the wind turbine in our case [13, 14, 17].

The following relation gives the evolution of the used power coefficient [2, 17]:

$$\begin{cases} C_p(\lambda,\beta)=C_1\left(\frac{C_2}{\lambda_i}-C_3\beta-C_4\right)e^{\frac{-C_5}{\lambda_i}}+C_6\lambda \\ \frac{1}{\lambda_i}=\frac{1}{\lambda+0.008\beta}-\frac{0.035}{\beta^3+1} \end{cases} \qquad (2)$$

Where β pitch angle, C1=0.5176; C2=116; C3=0.3; C4=5; C5=21; C6=0.0068 . [24] and incidence angle :

$$i = arctg\left(\frac{1}{\lambda}\right) = arctg\left(\frac{R\Omega}{V_1}\right) \qquad (3)$$

The well-known wind power equation for wind turbines is

$$P_m = \frac{1}{2}C_p(\lambda)\rho A V_1^3 \qquad (4)$$

Where Pm: the power captured by the wind turbine A: blade swept area [m2], λ: tip-speed ratio (specified speed), Cp: coefficient of power conversion, ρ: air density [kg/m3] and V1: a wind speed [m/s].

The factor of wind speed λ defined by:

$$\lambda = \frac{\Omega_t R_t}{V_1} \quad (5)$$

Where Rt : the radius of turbine blade [m], Ωt: rotating speed [rpm]. The torque of the wind power system can give with the following equation:

$$T_t = \frac{P_m}{\Omega_t} = \frac{1}{2}\rho\pi R^3 \frac{C_p(\beta,\lambda)}{\lambda} V^2 \quad (6)$$

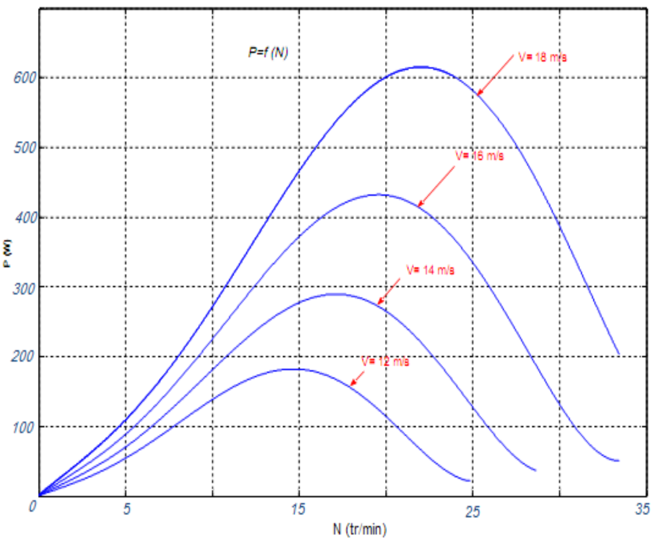

Figure .4 Wind power for various values of wind speed.

The value of the power coefficient Cp reaches the maximum at the particular λ named λopt. Hence, to maximize the extracted energy of wind turbine in MPPT zone, λ should be maintained at λopt, hence, the optimal rotor speed which is given by the Eq. (7), Fig.4, [13, 17].

$$\Omega_{ref} = \lambda_{opt}.V_t / R_t \quad (7)$$

For light winds (v < vN), control systems are designed to match the maximal power transfer point. This can be done by following the optimal tip-speed ratio, therefore obtaining the maximal Cp. For strong winds, regulation at PN is needed [15, 16].

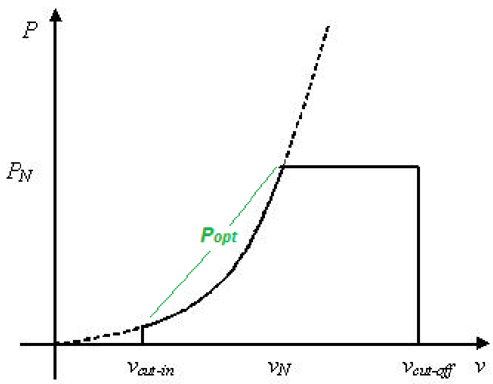

Figure .5 Functioning zones of the wind turbine [14].

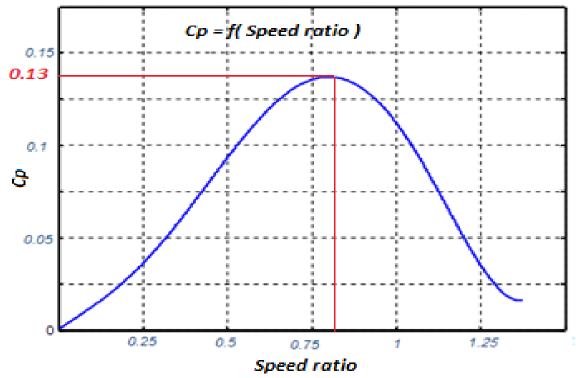

Figure .6 Characteristics retained for the tests of wind turbine.

The value of the pitch angle is kept constant at its smallest value (β = βmin= 2) in MPPT zone, where the wind power is less than nominal value, so the value of Cp becomes a function of λ and it reaches the maximum Cp=0.13) at the optimal tip speed ratio (λopt =0.85), Figure 6.

III. Generator PMSG model

The model of the generator PMSG is expressed at synchronous axes frame by, [3, 10, 17]:

$$\begin{cases} v_d = R_s . I_d + L_d \dfrac{dI_d}{dt} - L_q \omega I_q \\ v_q = R_s . I_q + L_q \dfrac{dI_q}{dt} + L_q \omega I_d + \phi_f \omega \end{cases} \quad (8)$$

where, v_{ds} ,v_{qs} : voltage of stator in (*d-q* axis), i_{ds} ,i_{qs} : current of stator in (*d-q* axis), L_d L_q : inductance in (*d-q* axis), R_s : stator resistance, ω : electric pulsation and Φ_f: magnetic flux of permanent magnet.

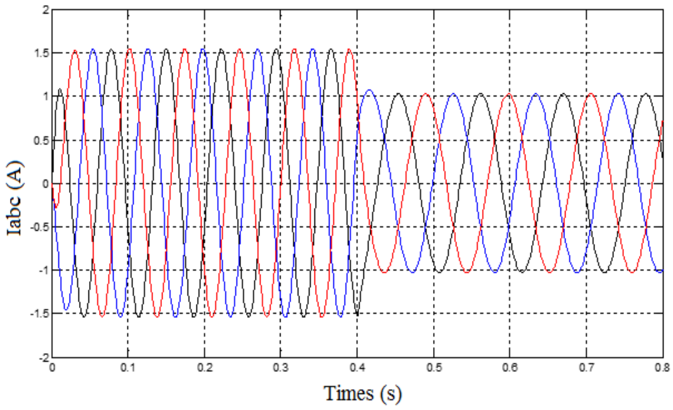

Figure .7 Stator current I_{abc} of PMSG after simulation.

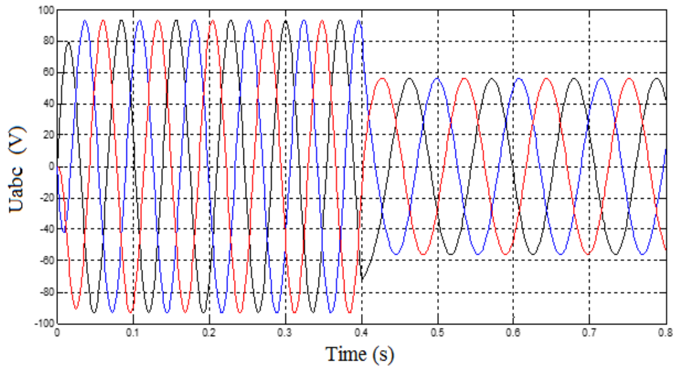

Figure .8 Stator tensions of PMSG after simulation.

The electromagnetic torque is given by [3, 17, 18, 19, 20]:

$$T_{em} = \frac{3}{2} p \left[\left(L_q - L_d \right) i_{ds} i_{qs} + i_{qs} \varphi_f \right] \qquad (9)$$

where, *p:* is the number of poles pairs.

After applying Field Oriented Control (FOC), *d*-axis is aligned with the magnetic flux, the final form of equation of T_{em}, like this:

$$T_{em} = \frac{3}{2} p . i_{qs} \varphi_f = K . i_{qs} \qquad (10)$$

After, we can use for the speed control of the generator the q axis current component. The d-axis current is set to (0) zero [8].
The mechanical system can be described as following relations, where T_t and T_a represent respectively the input wind torque and the torque before the gearbox:

$$T_t - T_a = J_t \frac{L d \Omega_t}{dt} + f_f \Omega_t \qquad (11)$$

Before the gearbox, the mechanical dynamics system can be described by relation (13) where T_b and T_g represents respectively the torque after the
gearbox
and the produced generator torque:

$$T_b - T_g = J_g \frac{L d \Omega_g}{dt} + f_g \Omega_g \qquad (12)$$

The transmission gearbox ratio is defined as:

$$G = \frac{\Omega_g}{\Omega_t} \qquad (13)$$

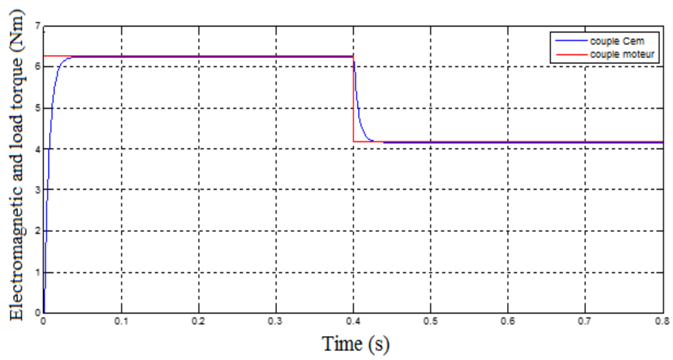

Figure .9 Electromagnetic & load torque of system.

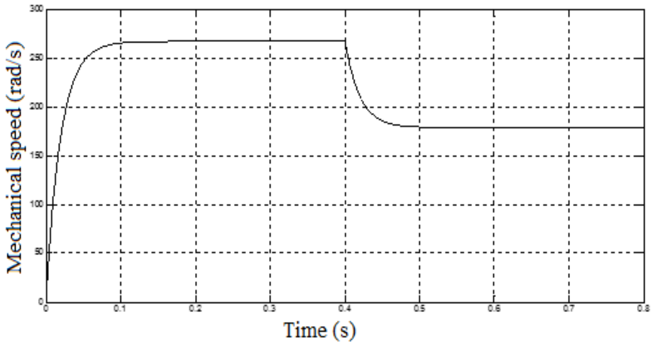

Figure .10 The speed of the generator

To chow the effect of the electric load on the generator as a function of the mechanical power supplied, two different motor torques are applied (fig.9). It is found that the speed of the generator is low and far from that of synchronism, which results in low voltages and currents shown in the figures (fig.7) and (fig.8). This is explained by the fact that the engine torque applied is insufficient. By decreasing the engine torque of 6.28Nm, at 4.2Nm, the mechanical speed varies from 267.60 rad / s to 178.9 rad / s. Voltage and current decrease respectively from 77.17V to 51.6V and from 1.54A to 1.03A. It is therefore clear that the electric power of the load is directly related to the mechanical power supplied.

The PWM rectifiers controlled by opening and closing semiconductors in a way allows obtaining the imposed references according to needs [3-17]. This rectifier controlled to keep the voltage of the continuous bus at a wished value of reference, by using a closed loop control.

Voltage equations of the three-phase system balanced without connection to neutral point can be written as follows [24]:

$$\begin{bmatrix} v_{sa} \\ v_{sb} \\ v_{sc} \end{bmatrix} = R_s \begin{bmatrix} i_{sa} \\ i_{sb} \\ i_{sc} \end{bmatrix} + L_s \frac{d}{dt} \begin{bmatrix} i_{sa} \\ i_{sb} \\ i_{sc} \end{bmatrix} + \begin{bmatrix} U_{sa} \\ U_{sb} \\ U_{sc} \end{bmatrix} \qquad (14)$$

$$C.\frac{dV_{dc}}{dt} = \left(S_a.i_a + S_b.i_b + S_c.i_c\right) - I_L \qquad (15)$$

Where:

$$\begin{cases} U_{sa} = \dfrac{2S_a - S_b - S_c}{3} V_{dc} \\ U_{sb} = \dfrac{2S_b - S_a - S_c}{3} V_{dc} \\ U_{sc} = \dfrac{2S_c - S_a - S_b}{3} V_{dc} \end{cases} \qquad (16)$$

IV. Control strategies for the generator

The wind turbine consists of the following components: A three-bladed rotor with the corresponding pitch angle controller, a PMSG with two back-to-back power converters a DC-Link capacitor, and a LC-filter. The control of the PMSG consists of the generator side control. The scheme of the wind turbine system is shown in Figure 2.

IV.1 Field Oriented Control “FOC”

The block diagram of the control is shown in the figure (Fig. 11). The reference electromagnetic torque T_g may be designed for fixed power operation which is in any case used to limit the power of the PMSG generator to its nominal value. As a result, the vector control technique will be used.

There are several strategies for vector control of permanent magnet synchronous machines depending on how the electromagnetic torque is produced [3, 7, 8]. In this case, we present the PMSG vector control for current regulation. This topology allows a better dynamic in the control of the torque while avoiding the disadvantages of a power supply.

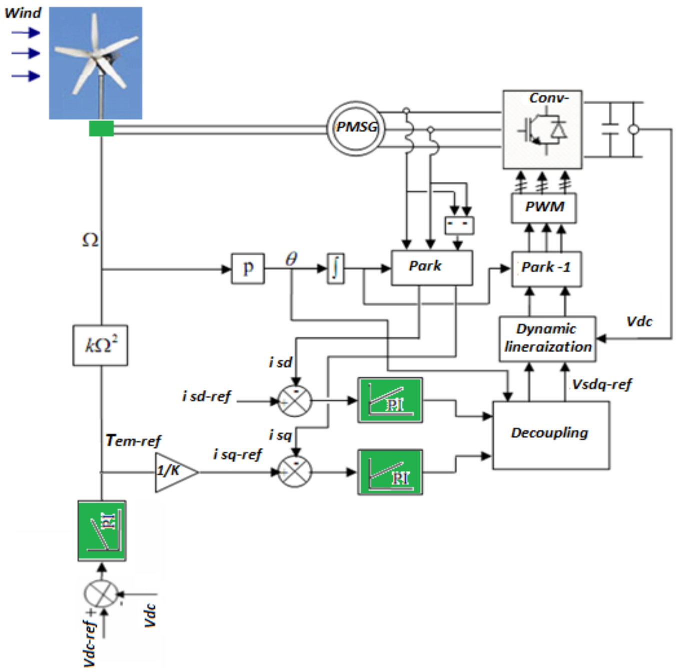

Figure .11 Block diagram of Field Oriented Control

Since the torque control depends on the two variables I_d and I_q, the main objective of the vector control of the PMSG is to control the torque according to a chosen criterion. The criterion chosen often corresponds to the minimization of Joule losses at given torque. However, this criterion requires simultaneous control of the currents I_d and I_q. To simplify the control, the current Id is often fixed so that the torque is proportional to I_q in a given speed range.

The machine is designed with salient poles, the electromagnetic torque is maximum when the stator current in the repository Park is kept locked on the axis q ($I_s = I_q$). This amounts to imposing the direct component of the zero current, which has the effect of reducing joule losses. The system of equations becomes:

$$\begin{cases} v_d = -L_q \omega I_q \\ v_q = R_s . Iq + L_q \dfrac{dI_q}{dt} + \phi_f \omega \end{cases} \quad (17)$$

It is proposed to implement PI-type regulators in the control structure. The equations of the mathematical model of the permanent magnet synchronous machine can be written by the following form:

$$\begin{cases} v_d = R I_d + L_d \; s \; I_d - L_q \omega I_q \\ v_q = R \; I_q + L_q \; s \; I_q + L_d \; \omega \; I_d + \omega \varphi_f \end{cases} \quad (18)$$

s: Laplace operator.

We can define the terms of coupling functions: F_{emd} and F_{emq}. The voltages after compensation each v_{d1} and v_{q1} have a first-order relation proportional to the corresponding current.

$$\begin{cases} F_{emd} = \omega \, . \, L_d \, . \, I_q \\ F_{emq} = \omega \, . (L_d \, . \, I_d + \phi_f) \end{cases} \quad (19)$$

And;

$$\begin{cases} v_{d1} = L_d \cdot \frac{d\,I_d}{dt} + R \cdot I_d \\ v_{q1} = L_q \cdot \frac{d\,I_s}{dt} + R \cdot I_q \end{cases} \quad (20)$$

Thus, equations (20) are written with the new command variables v_{dl} and v_{ql} as follows:

$$\begin{cases} v_d = v_{d1} - F_{emd} \\ v_q = v_{q1} + F_{emq} \end{cases} \quad (21)$$

The current Id depends only on v_{dl} and Iq depends only on v_{ql}. Their expressions are written as follows:

$$\begin{cases} I_d = \frac{v_{dl}}{R + L_d.s} \\ I_q = \frac{v_{ql}}{R + L_d.s} \end{cases} \quad (22)$$

We consider that the machine is vector-oriented and completely decoupled. This allows us to write the equations of the machine in a simple way and to calculate the coefficients of the regulators.

For the current loops, we propose classical regulators Proportional Integrator (P.I). They comprise a proportional action, which serves to regulate the speed and to eliminate the static error between the regulated variable and the reference variable.

The regulator is written in the following form:

$$P.I \rightarrow \frac{U_r}{\varepsilon} = \frac{1 + sT_1}{sT_2} \quad (22)$$

Where,

$$\begin{cases} U_r = (K_p + \frac{K_i}{s}) \\ K_p = \frac{T_1}{T_2} \quad et\, K_i = \frac{1}{T_2} \end{cases} \quad (23)$$

Controlling the torque PMSG is based on the simultaneous control of two variables I_d and I_q. The system consists of a torque control loop that imposes the reference current I_q. The current I_d is kept zero. To have zero static error, P.I regulators perform to the control. According to equation (23) and the regulation structure, we obtain the diagram of the figure (fig. 12).

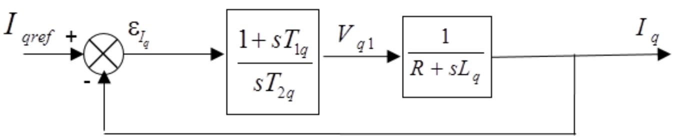

Figure .12 Control current loop I_q.

The open loop transfer function is given by the following equation:

$$FT_{bo} = \frac{1 + sT_{1q}}{T_{2q}.s(R + sL_q)} \quad (24)$$

The following practical set-up time is usually taken as follows: $tr = 3.\tau_q$ *(Critère de ± 5%)*

$$\tau_q = R_S.T_{2q} \quad \Rightarrow \quad T_{2q} = \frac{\tau_q}{R_S} = \frac{tr}{3\,.R_S} \quad (25)$$

where, t_r: response time imposed (t_r = 5ms) and τ_q : Electrical time constant of the axis "q".

After that, to regulate the DC bus voltage Vdc, consider the following diagram, which implements the voltage and current loops in cascade.

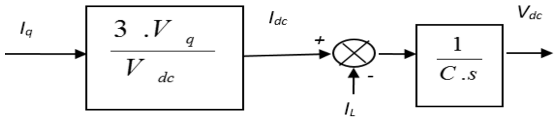

Figure .13 Model of the voltage loop

The global structure of the closed-loop system is shown in Figure (Fig. 14):

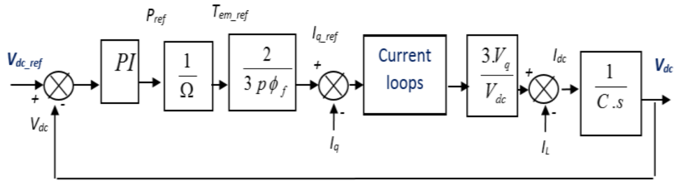

Figure .14 Global model for voltage regulation.

To determine the parameters (*Kc*, *Tc*) of the corrector PI, the function of system is compared with the characteristic function:

$$H_{BF}(s)=\frac{1+T_c s}{\frac{CT_c}{GK_c}s^2+T_c s+1}=\frac{1+T_n s}{\frac{1}{\omega^2{}_n}s^2+\frac{2\varepsilon}{\omega_n}s+1} \tag{26}$$

Where,

$$K_c=\frac{2CV_{dc}\omega_n}{3e_g} \quad \text{and} \quad T_c=\frac{2\varepsilon}{\omega_n}$$

The bandwidth of the voltage regulator is fixed relative to the frequency of the electromotive force of PMSG therefore depends directly on the speed of the alternator.
Typically it takes, ε = 0,7 and ω_n = 0,1 ω_{mes}.

IV. Direct Power Control "DPC"

In this case, the controllers used are hysteresis comparators for the mistakes of active and reactive power instantaneous (Δq, Δp). The output regulators with the sector where the place of the vector voltage of PMSG, constitute the inputs of a switch panel which in turn determines the switching state of the switches, the active power reference is obtained from controller of bus voltage [4, 25]. The power calculation, instantaneous active and reactive, is given by the following equations:

$$p=U_{dc}(S_a i_a+S_b i_b+S_c i_c)+L\left(\frac{di_a}{dt}.i_a+\frac{di_b}{dt}.i_b+\frac{di_c}{dt}.i_c\right) \tag{27}$$

$$q=\frac{1}{\sqrt{3}}\left\{-U_{dc}\left[S_a(i_b-i_c)+S_b(i_c-i_a)+S_c(i_a-i_b)\right]+3L\left(\frac{di_a}{dt}.i_c-\frac{di_c}{dt}.i_a\right)\right\}$$

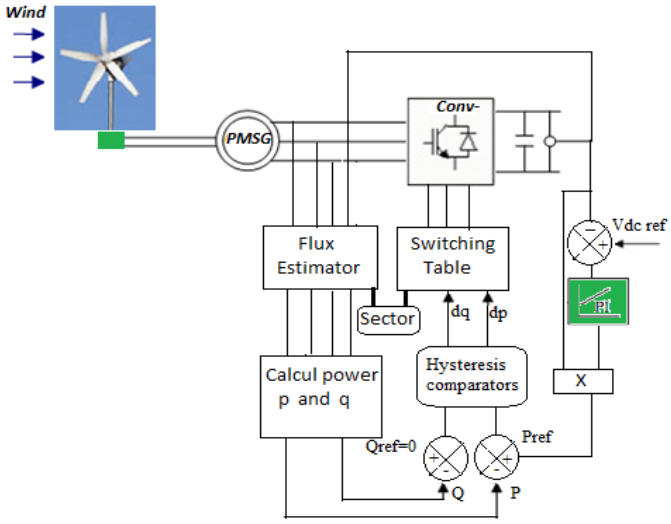

Figure .15 Block diagram of direct power control.

V. Comparative study of DPC and FOC control of PMSG

The wind turbine system based on the permanent magnet synchronous generator controlled by vector PWM rectifier was studied by simulation under Matlab / Simulink.

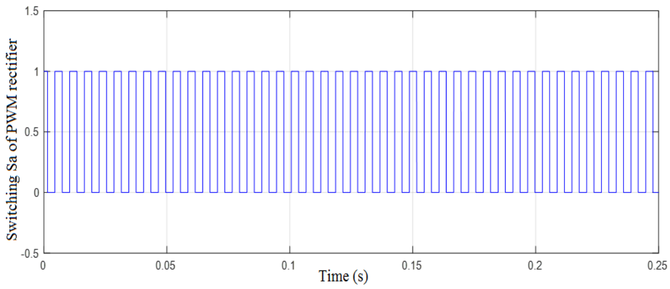

Figure .16 Switching state S_a of the of the PWM rectifier switches

The current was controlled in the *abc* reference by hysteresis regulators, the reference of the voltage at the output of the rectifier is taken equal to 45.8 V.

We simulated the wind profile model in two forms:

- The wind speed is shown in Simulink by the figure (Fig.16). Depending on the position of the manual switch in the diagram, the wind speed is considered as a velocity with a turbulence component. This turbulence component is generated by the filtering of a pseudo random noise.

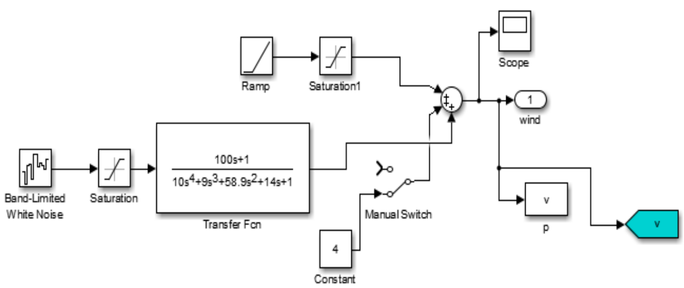

Figure .17 Diagram under Matlab-Simulink of wind speed.

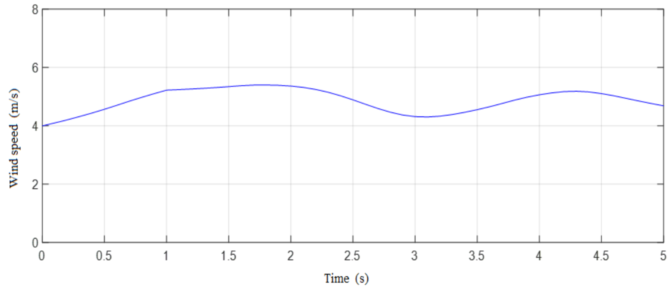

Figure .18 Wind speed simulation

- The variation of wind speed shown in figure (Fig. 19) are modeled in deterministic form by a sum of several harmonics [3, 4, 9, 10, 13] in the equations (1).

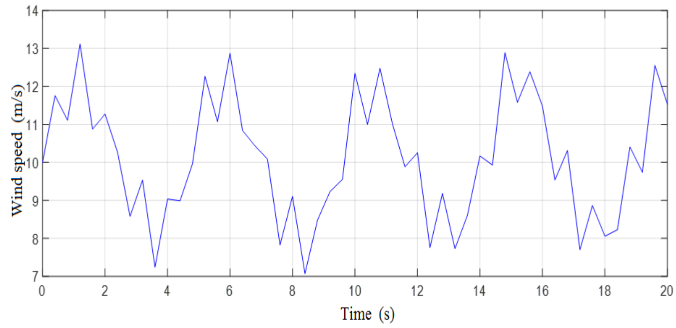

Figure .19 Wind speed as a function of time

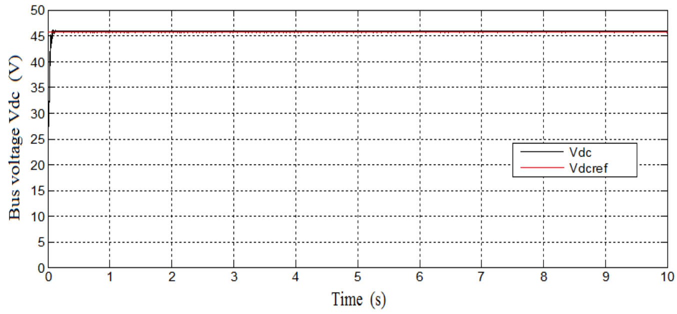

Figure .10 Bus voltage of system after FOC technique

The simulation results obtained after application FOC control, show that the response of the voltage at the rectifier output (rectified) to a speed variation is relatively fast and does not exceed 1% of the reference value during disturbances.

It is clear that with the application of the two proposed models of wind speed (Figures 18 and 19), the pace of the DC bus voltage is established at 45.8V with a response time which depends on the control of the rectifier, in the order of 0.5 s of the example being processed.

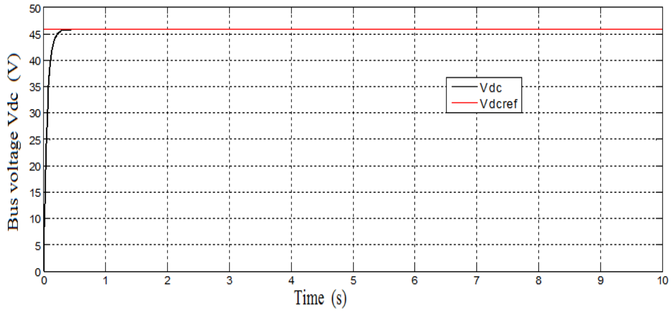

Figure .11 DC bus voltage and reference after DPC technique

The figure (Fig.21) shows the DC voltage at the output of the rectifier after application control DPC, it is observed that the DC bus voltage remains on average equal to the proposed reference 45.8 V. It is observed that the DC bus voltage (Fig. 21) remains on average equal to 45.8V. The wind speed profile is the cause of the bus voltage fluctuations. Indeed, when the wind speed varies the rectifier control must follow the change of the operating point in order to stabilize the bus voltage.

Steady-state simulations show that the best power quality features and the smaller DC voltage error are given by the FOC technique. On the other hand, DPC technique otters the tastest transient behavior without overshoot (~3%). Table 1 shows a brief description of simulation results along with the characteristics of each control strategies.

Table 1. Comparison between the performance indices of the rectified voltage for different controllers studied.

Control strategies	**FOC**	**DPC**
Modulation	PWM	Hysteresis
Tracking Error	0.65 %	5.53 %
Setting time	<160 ms	<130 ms
Rise time	<30 ms	<20 ms
Overshoot	~13 %	~3 %
Zoom of bus voltage V_{dc} and the reference	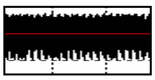	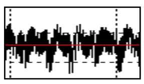

VI. Conclusion

This paper has presented a modeling technique and a control method proposed for small wind energy conversion system.

The describes and analysis of two different control strategies for PMSG have been carried out. The results of this comparative study show that both control strategies can be used to control small wind turbines. However, the best power quality features and the smaller DC voltage error are obtained with FOC control techniques. On the other hand, DPC control offers the better dynamic response without overshoot.

We conclude that the FOC control is better as adapted on the wind system, and is more efficient than DPC control.

References

[1] Feifei Bu, Yuwen Hu, Wenxin Huang, Shenglun Zhuang, Kai Shi.Wide-Speed-Range-Operation Dual Stator-Winding Induction Generator DC Generating System for Wind Power Applications. IEEE Transactions On Power Electronics, Vol. 30, No. 2, pp. 561-573, February 2015.

[2] Ye Wang, Herman Bayem, Maria Giralt-Devant, Vera Silva, Xavier Guillaud, Bruno Francois. Methods for Assessing Available Wind Primary Power Reserve. IEEE Transactions On Sustainable Energy, Vol. 6, No. 1, pp.272-280, January 2015.

[3] Eduardo Giraldo, Alejandro Garces. An Adaptive Control Strategy for a Wind Energy Conversion System Based on PWM-CSC and PMSG. IEEE Transactions On Power Systems, Vol. 29, No. 3, pp. 1446-1453, May 2014.

[4] A. Harrouz, I. Colak, K. Kayisili, " Control of a Small Wind Turbine System Application," IEEE Explore, the 5th International Conference on Renewable Energy Research and Applications (ICRERA) 2016, Birmingham, UK. 20-23, November 2016.

[5] Mazhar Hussain Baloch, Jie Wang, Ghulam Sarwar Kaloi, "Dynamic Modeling and Control of Wind Turbine Scheme Based on Cage Generator for Power System Stability Studies." International Journal of Renewable Energy Research-IJRER, Vol 6, No 2 , 2016.

[6] Dileep Kumar Varma, Obulesh YP, Saibababu ch " An Improved Synchronous Reference Frame Controller based Dynamic Voltage Restorer for Grid Connected Wind Energy System." International Journal of Renewable Energy Research-IJRER, Vol 6, No 2 , 2016.

[7] Mehdi Allagui; OthmanBk Hasnaoui; Jamel Belhadj, "A 2MW direct drive wind turbine; vector control and direct torque control techniques comparison", J. energy South. Afr. vol.25 n.2 Cape Town, ISSN: 2413-3051, May 2014.

[8] A. Harrouz, H Becheri, I Colak, K Kayisli, "Backstepping control of a separately excited DC motor", Electrical Engineering, Springer Berlin Heidelberg , ISSN: 0948-7921, Vol.99, Issue 3, pp.1-11, June 2017.

[9] Salvador Alepuz, Alejandro Calle, Sergio Busquets-Monge, Samir Kouro, Bin Wu, "Use of Stored Energy in PMSG Rotor Inertia for Low-Voltage Ride-Through in Back-to-Back NPC Converter-Based Wind Power Systems". IEEE Transactions On Industrial Electronics, Vol. 60, No. 5, pp. 1787-1796, May 2013.

[10] Giampaolo Buticchi, Emilio Lorenzani, Member, Fabio Immovilli, Claudio Bianchini. Active Rectifier With Integrated System Control for Micro wind Power Systems. IEEE Transactions On Sustainable Energy, Vol. 6, No. 1, pp. 1-10, January 2015.

[11] Nuno M. A. Freire, Jorge O. Estima, António J. Marques Cardoso. "A New Approach for Current Sensor Fault Diagnosis in PMSG Drives for Wind Energy Conversion Systems", IEEE Transactions On Industry Applications, Vol. 50, No. 2, pp. 1206-1214, April 2014.

[12] Marius Fatu, Frede Blaabjerg, Ion Boldea. Grid to Standalone Transition Motion Sensorless Dual-Inverter Control of PMSG With Asymmetrical Grid Voltage Sags and Harmonics Filtering. IEEE Transactions On Powers Electronics, Vol. 29, No. 7, pp. 3463-3472, July 2014.

[13] H. Glaoui, A. Harrouz, I. Messaoudi, H. Saab, "Modelling of Wind Energy on Isolated Area", International Journal of Power Electronics and Drive System (IJPEDS), ISSN: 2088-8694, Vol. (4) No.2, pp. 274-280, Juin 2014.

[14] Marwan Rosyadi, S. M. Muyeen, Rion Takahashi, Junji Tamura, Fuzzy-PI Controller Design for PM Wind Generator to Improve Fault Ride Through of Wind Farm", International Journal of Renewable Energy Research-IJRER, Vol 3, No 2, 2013.

[15] Dinesh Kumar Yadav, T. S. Bhatti, Ashu Verma "Study of Integrated Rural Electrification System Using Wind-Biogas Based Hybrid System and Limited Grid Supply System", International Journal of Renewable Energy Research-IJRER, Vol 7, No 1, 2017.

[16] Jianxing Liu, Salah Laghrouche, Mohamed Harmouche , Maxime Wack, "Adaptive-gain second-order sliding mode observer design for switching power converters", Energy Conversion and Management, Volume 30, Issue , Pages 124-131, January 2014.

[17] Muhammad Hamid Mughal; Li Guojie, “Review of Pitch Control for Variable Speed Wind Turbine,” IEEE Explore, 15th Intl Conf on Scalable Computing and Communications and Its Associated Workshops (UIC-ATC-ScalCom), Pages: 738 – 744, 2015.

[18] N. Nakasone, T. Senjyu, A. Yona, A. T. Saber, Funabashi and H. Sekine. Operation strategies for stability of gearless wind power generation systems. IEEE conference, Power and Energy Society General Meeting, Conversion and Delivery of Electrical Energy in the 21 st Centry, pp.1-7, 2008.

[19] S. Ganjefar, A. A. Ghassemi, M. M. Ahmadi. Improving efficiency of two-type maximum power point tracking methods of tip-speed ratio and optimum torque in wind turbine system using a quantum neural network. Energy, Vol (67): pp. 444-453, 2014.

[20] Nikolay Djagarov ; Zhivko Grozdev ; Milen Bonev ; Julia Djagarova ; Andrey Pazderin ; Sergey Kokin, " Adaptive control of wind PMSG". 17th International Scientific Conference on Electric Power Engineering (EPE), 2016.

[21] Hanzo L. Power conversion and control of wind energy systems. IEEE press; Edition 2011.

[22] M. Montero. E. Cadaval. V. Marcos. M. Martinez. Three-phase PWAI Sinusoidal Current Rectifier with Power Conditioning Capability. 35th Annual Conference of IEEE Industrial Electronics. IECON 09. Porto. Portugal. pp. 3703 - 3708. 2009.

[23] http://circuitglobe.com/permanent-magnet-dc-motor.html;

[24] Thomas Ackermann, Wind Power in Power systems, Royal Institute of Technology Stockholm, Sweden, 2015.

[25] Mohamed nader amrani, Abderrahmane Dib, “Predictive Direct Power Control of a Grid Connected Three-Phase Voltage Source Inverter for Photovoltaic Systems”, International Journal of Renewable Energy Research-IJRER, Vol 6, No 1 , 2016.